Metamaterial Structure Based Dual-Band Antenna for WLAN

Xueqi Wu, Xi Wen, Jing Yang, Shaolong Yang, and Jianchun Xu

***Abstract*—With the development of communication technology and the wide application of 5G information technology, various mobile equipment manufacturers have higher demands for compact, small, light, low-cost, and dual-band antennas. Therefore, this paper designs a metamaterial structure-based antenna with operating frequencies covering the wireless local area network (WLAN) bands. According to the simulated and measured results, the bandwidths of the antenna below −10 dB include 2.326 − 2.859 GHz and 4.995 − 5.854 GHz. The measured results are in good agreement with the simulated ones. Moreover, the radiation energy of the proposed antenna is relatively concentrated, and the gain can reach 3.5 dBi and 3.53 dBi at the center frequencies of two operating bands. All the results show that a novel CPW-fed antenna with compact structure, low cost, and dual-band is successfully implemented.**

***Index Terms*—Antenna, CPW, dual-band, metamaterial.**

I. Introduction

WIRELESS local area network (WLAN) based on the IEEE 802.11 standards, also commonly called Wi-Fi, is widely used in network media, daily life, and other terminal equipment [1], [2]. In the fifth generation (5G) mobile communication system, the WLAN supports both low and high frequency bands of 2.400 GHz − 2.484 GHz (2.4 G band) and 5.150 GHz − 5.825 GHz (5G band) [3]–[5]. The low frequency band has small transmission attenuation and long transmission distance [6], which satisfies the requirements of signal coverage and capacity. The high frequency band has wide bandwidth and stable network speed [7], the signal capacity can be increased where access point is concentrated. Antennas used to transmit and receive electromagnetic waves for wireless equipment are an important part of Wi-Fi systems [8]–[10].

In recent years, the popularity of intelligent terminal products promotes the development of wireless voice, Bluetooth data transmission, etc [11]–[13]. And almost all terminal devices are optimized for miniaturization. Therefore, the demands for compact [14], [15], low-cost [16], [17], light weight [18] and multiband antennas [19]–[21] are increasing. With the rapid development of microstrip circuits [22], [23], a coplanar waveguide circuit [24]–[26] is proposed for the miniaturization of the antennas. The CPW circuit has the advantages of low dispersion, low loss, and easy integration. Therefore, the CPW feed technology [27] in the antenna design inherits these advantages in wireless communication systems. Single-frequency antennas based on CPW or other structures emerge endlessly [28]–[30]. The antennas working in a single-band will not only produce electromagnetic interference [31]–[33] and reduce the compatibility [34], but also bring the problems of larger size and high cost of terminal products. Therefore, it is necessary to design multi-band antennas to reduce the interference and size. Metamaterial [35]–[36] is a kind of man-made material that uses metal coils, wires, split-ring resonators (SRRs) and other artificial ways to create reactions to electric and magnetic fields, so it has electromagnetic properties that natural materials do not have. In this paper, split ring resonators were connected at the end of feeder line due to their ability to produce strong electromagnetic resonances. Therefore, this metamaterial structure is used in our design.

Here, a CPW-fed dual-band antenna with metamaterial structure is presented for improving the spectrum utilization efficiency. The antenna configuration is introduced, and the main parameters that could affect the bandwidth of the antenna are studied. In order to demonstrate the design concept, a dual-band antenna prototype is designed, manufactured, and tested. According to the simulated and measured results, the antenna can achieve full radiation coverage to 2.4G and 5G-WLAN bands. Measured and simulated results well coincide with each other.

II. Antenna Design

The geometry of the proposed antenna is shown in Fig. 1. The resonant structure made of copper was fabricated on an FR-4 dielectric substrate with a thickness of 2 mm, a relative permittivity of 2.65, and a permeability of 1. The proposed antenna adopted CPW feed technology, and the length and width of the feeder line are $h_1 = 27$ mm and $w = 2$ mm. SRRs were connected at the end of the feeder line due to their outstanding miniaturization potentialities and ability to produce strong electromagnetic resonances. From Fig. 1, the side length and width of the SRRs are $c = 13$ mm and $w_1 = 1$ mm, and

Manuscript received March 8, 2022; revised March 22, 2022; accepted March 25, 2022. Date of publication March 29, 2022; date of current version April 13, 2022. This work was supported in part by the National Natural Science Foundation of China under Grant 52102061, in part by the Beijing Youth Top-Notch Talent Support Program, and in part by the Science and Technology Plan of Shenzhen City under Grants JCYJ20180306173235924 and JCYJ20180305164708625. *(Corresponding author: Jianchun Xu.)*

Xueqi Wu, Jing Yang, Shaolong Yang, and Jianchun Xu are with the State Key Laboratory of Information Photonics and Optical Communications & School of Science, Beijing University of Posts Telecommunications, Beijing 100876, China, and also with the Beijing University of Posts and Telecommunications Research Institute, Shenzhen 518057, China (e-mail: wuxueqi@bupt.edu.cn; trancyj@bupt.edu.cn; yangshaolong@bupt.edu.cn; jianchun_xu@bupt.edu.cn).

Xi Wen is with the School of Mechanical Engineering, Nanjing University of Science and Technology, Nanjing 210094, China (e-mail: 15201615855@163.com).

Digital Object Identifier 10.1109/JPHOT.2022.3163170

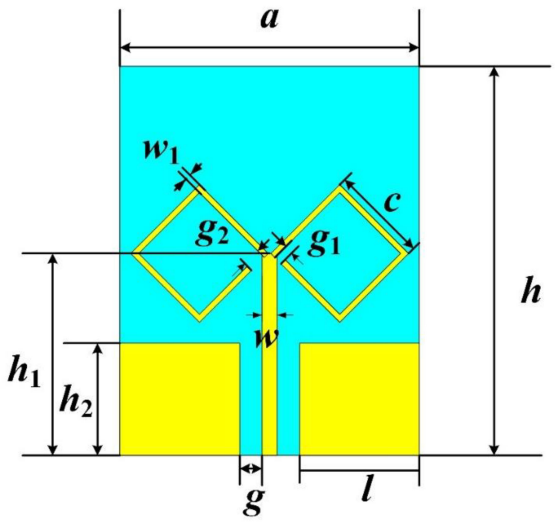

Fig. 1. Geometry of the proposed antenna.

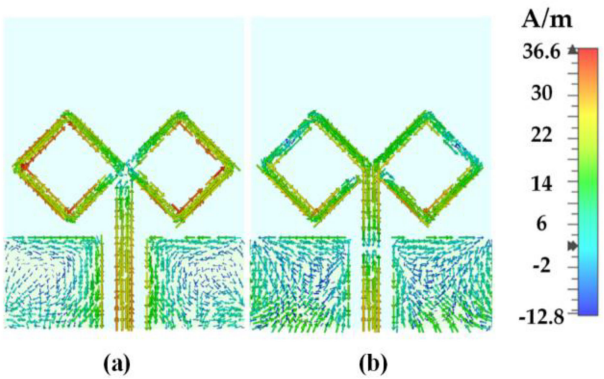

Fig. 2. Current distributions of the CPW antenna at (a) 2.5 GHz and (b) 5.5 GHz.

the gap widths of the splits are $g_1 = 1$ mm and $g_2 = 2$ mm. The other structure parameters are as follows: $l = 15$ mm, $h_2 = 16$ mm, $g = 2$ mm. The total size of this compact antenna is 40 mm $\times$ 52 mm.

Numerical predictions of the reflection coefficients for the proposed antenna were made using the CST Microwave Studio. To investigate the structure parameters that influence the electromagnetic characteristics of the proposed antenna, the simulated surface current distributions at 2.5 GHz and 5.5 GHz are shown in Fig. 2. At 2.5 GHz, the current, as shown in Fig. 2a, is mainly distributed on both sides of the feeder line and SRRs. The effective current length starts from the bottom of the grounding plate. This effective current length is longer, the proposed CPW antenna operates in the low frequency band of 2.5 GHz. From Fig. 2b, the effective currents on the feeder and SRRs are discontinuous at 5.5 GHz. The effective current obtains shorter length, generating electromagnetic resonance at high frequency. Based on these two kinds of resonant modes, the characteristic of the two operating bands is realized. The above analysis indicates that the side length c, and width w_1 of the SRRs, and length h_1 and width w of the connecting feeder have a crucial impact on the radiation performance of the antenna in the operating bands. By reasonably adjusting the structure parameters of the radiation unit, the full coverage of all Wi-Fi bands can be finally achieved.

To substantiate this size effect, the reflection coefficients of the proposed CPW antenna are explored. The simulated curves in Fig. 3 exhibit two resonant peaks, the center frequency of the first resonant peak is near 2.5 GHz, and the second one is close to 5.5 GHz. The dotted lines indicate the start and stop frequencies of the two WLAN bands. As shown in Fig. 3a, the two resonance peaks of the antenna shift to low frequency when the side length c of the SRRs increases from 11 mm to 14 mm. As $c = 13$ mm, the CPW antenna can realize dual-band radiation and completely cover the 5G-WLAN band. From Fig. 3b, with the increase of feeder length h_1, the resonant frequencies of the proposed dual-band antenna have red-shift. This parameter can gravely influence the operating band of the design CPW antenna.

As the width w_1 of SRRs was changed from 0.6 mm to 1.2 mm with 0.2 mm intervals, the operating bands of CPW antenna have blue-shift as depicted in Fig. 3c. Except for the feeder length, it is also necessary to discuss the influence of feeder width on antenna performance. When the width w of the feeder line increases from 1 mm to 2.5 mm, the first resonant peak shifts to low frequency, and the second resonant peak moves to high frequency first and then to low frequency. As drawn in Fig. 3d, when $w = 2$ mm, the operating bands can perfectly cover the WLAN bands.

By changing the structure parameters of the CPW antenna, the bandwidth of the antenna can be adjusted effectively. Variation of the side length and width show a coincident impact on the two resonance peaks of the antenna. In particular, variations of the length and width of the feeder line can individually control the resonance peaks of the antenna. From the above simulations and analysis, the bandwidth and resonance peaks of the antenna can be controlled by opting the adequate structural parameters. Finally, the operating bands of the proposed CPW antenna can completely cover the WLAN band after optimizations.

III. Results and Discussions

To verify the practical electromagnetic performance of the proposed antenna, a fabricated CPW antenna is shown in Fig. 4. The reflection coefficients of the antenna are measured by a vector network analyzer. From Fig. 5, the measured -10 dB bandwidth of the proposed CPW antenna is $2.164 - 2.638$ GHz and $4.48 - 5.812$ GHz. The simulated operating bands of the proposed CPW antenna include $2.326 - 2.859$ GHz and $4.995 - 5.854$ GHz. These simulation and measurement results have acceptable consistency and confirm the reasonability of this design.

Radiation characteristics of CPW antenna in E-plane and H-plane at 2.44 GHz and 5.5 GHz are simulated and measured. These results are illustrated in Fig. 6. The radiation main lobe of the antenna is along the negative direction of the z-axis, and the max gain is 3.24 dBi at 2.44 GHz. Similarly, the radiation pattern in H-plane is not omnidirectional and exhibits a bidirectional pattern with a max gain of 3.5 dBi. At 5.5 GHz, the proposed antenna also exhibits a bidirectional pattern in E-plane, and the max

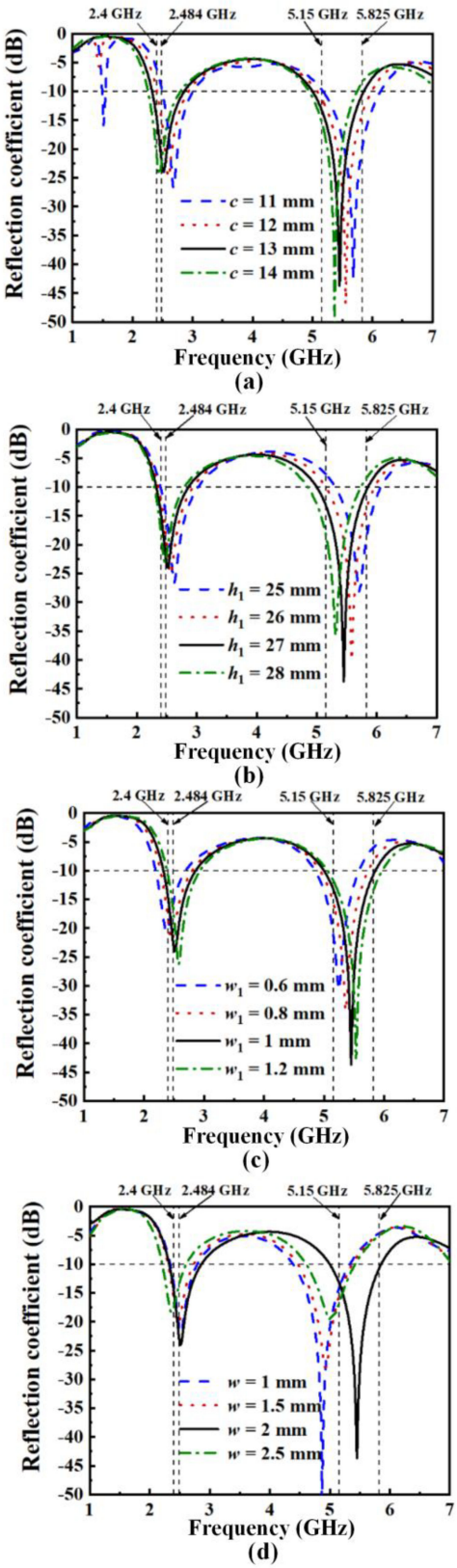

Fig. 3. Simulated reflection coefficient curves with various parameters of (a) c, (b) h_1, (c) w_1, and (d) w.

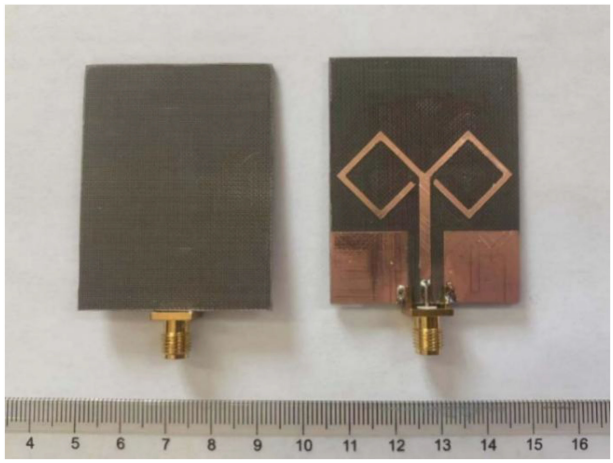

Fig. 4. Photograph of the fabricated antenna.

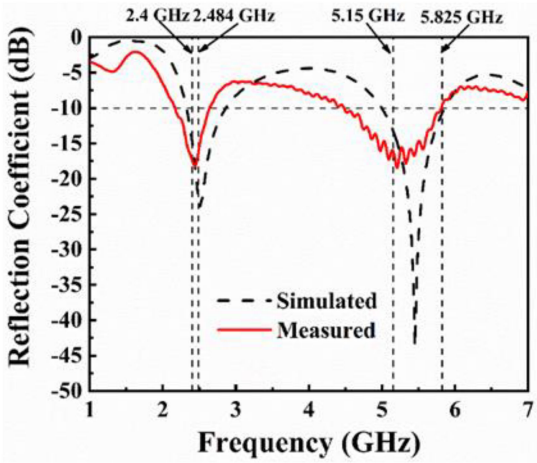

Fig. 5. Simulated and measured reflection coefficient curves of the proposed antenna.

TABLE I
COMPARISON BETWEEN PROPOSED AND REFERENCED ANTENNAS

Structure	Dimension (mm)	-10 dB Bandwidth(GHz)	Relative Bandwidth(%)	Gain(dBi)
Proposed	40 × 52	2.326-2.859	20.6	3.50
		4.995-5.845	15.7	3.53
[37]	40 × 35	2.38-2.52	5.7	2.2-2.7
		4.86-6.87	34.2	2.0-3.0
[38]	32 × 16	2.252-2.540	12.0	2.8
		4.855-7.212	39.0	4.29
[39]	40 × 35	2.12-2.77	26.6	1.87
		4.91-5.50	11.3	2.88

gain of the antenna reaches 3.53 dBi. These results demonstrate the good directivity of the proposed CPW antenna in operating bands, and their radiation energy is relatively concentrated.

Table I shows the comparison between the proposed antenna and some other Wi-Fi antennas. From this Table, it can be seen that our design has excellent performance in gain and relative bandwidth.

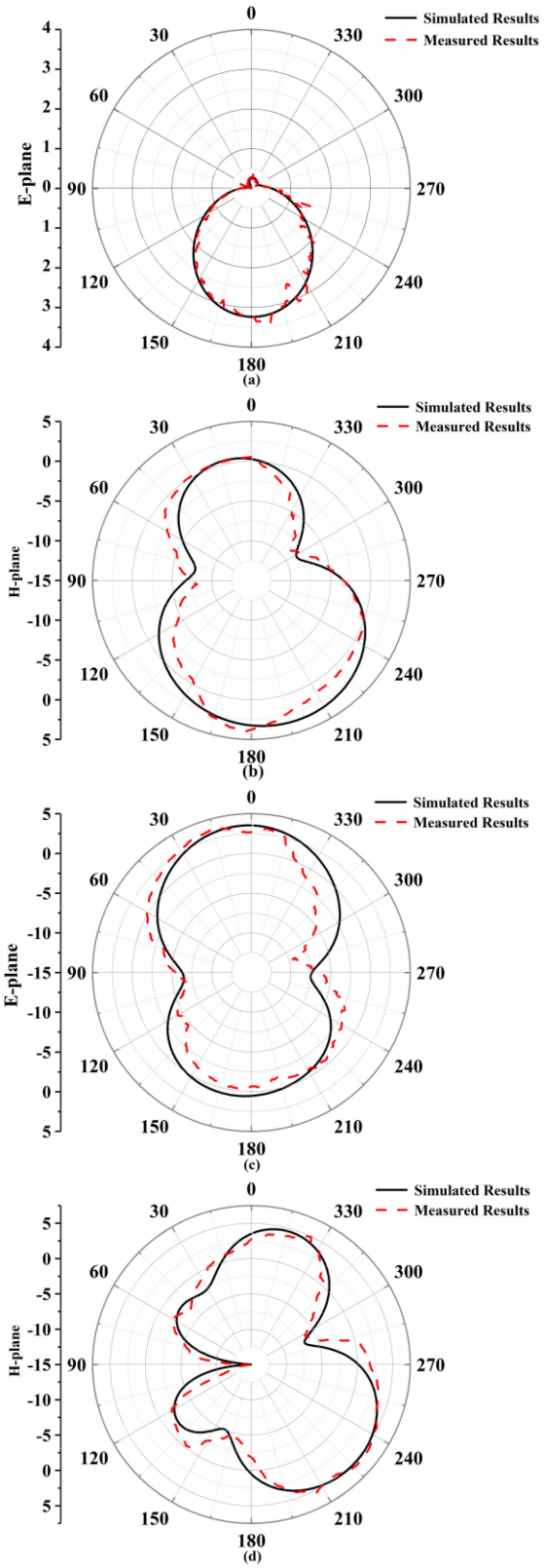

Fig. 6. Simulated and measured patterns of the antenna: (a) 2.44 GHz in E-plane, (b) 2.44 GHz in H-plane, (c) 5.5 GHz in E-plane, (d) 5.5 GHz in H-plane.

IV. Conclusion

A CPW dual-band antenna with metamaterial structure is proposed in this paper. The simulated results show that the bandwidth and resonant frequencies of the antenna can be adjusted by changing the structure parameters of the feeder line and the SRRs. Based on the variation regulation, a dual-band CPW antenna that can operate at whole WLAN bands is finally obtained. From simulated and measured results, the acceptable consistency demonstrates the practical effect of the proposed antenna. According to the E-plane and H-plane patterns of the antenna, the antenna exhibits good directivity and gain.

References

[1] H. Du *et al.*, "Research progress in broadband absorber based on artificial electromagnetic medium," *J. Mater. Eng.*, vol. 48, no. 6, pp. 23–33, 2020.
[2] Y. Cao, S. Cheung, and T. I. Yuk, "A multiband slot antenna for GPS/WiMAX/WLAN systems," *IEEE Trans. Antennas Propag.*, vol. 63, no. 6, pp. 952–958, Mar. 2015.
[3] H. Wu *et al.*, "Research progress in hyperbolic metamaterials and sensors," *J. Mater. Eng.*, vol. 48, no. 6, pp. 34–42, 2020.
[4] M. Yassin *et al.*, "Single-fed 4G/5G multiband 2.4/5.5/28 GHz antenna," *IET Microw., Antennas Propag.*, vol. 13, pp. 286–290, 2019.
[5] H. Bong *et al.*, "Design of an UWB antenna with two slits for 5G/WLAN-notched bands," *Microw. Opt. Technol. Lett.*, vol. 61, pp. 1295–1300, 2019.
[6] H. Guo *et al.*, "Ferromagnetic/ferroelectric composites and microwave properties of its metamaterial structure," *J. Mater. Eng.*, vol. 48, no. 6, pp. 43–49, 2020.
[7] R. V. Nee, "Breaking the gigabit-per-second barrier with 802.11 AC," *IEEE Wireless Commun.*, vol. 18, no. 2, Apr. 2011, Art. no. 4.
[8] H. Yao *et al.*, "Dual-band microstrip antenna based on polarization conversion metasurface structure," *Front. Phys*, vol. 8, 2020, Art. no. 279.
[9] J. Xu *et al.*, "A small-divergence-angle orbital angular momentum metasurface antenna," *Research*, vol. 2019, 2019, Art. no. 9686213.
[10] H. Zhang *et al.*, "Design of a tunable omnidirectional circularly polarized antenna based on VO_2," *Int. J. RF Microw. Comput.-Aided Eng.*, vol. 30, 2020, Art. no. e21997.
[11] X. Liu *et al.*, "Infrared stealth metamaterials," *J. Mater. Eng.*, vol. 48, no. 6, pp. 1–11, 2020.
[12] Y. Ampatzidis *et al.*, "Voice-controlled and wireless solid set canopy delivery VCW-SSCD system for mist-cooling," *Sustainability*, vol. 10, pp. 421, 2018.
[13] E. Park *et al.*, "AdaptaBLE: Adaptive control of data rate, transmission power, and connection interval in bluetooth low energy," *Comput. Netw.*, vol. 181, 2020, Art. no. 107520.
[14] M. Zaeimbashi *et al.*, "Ultra-compact dual-band smart NEMS magnetoelectric antennas for simultaneous wireless energy harvesting and magnetic field sensing," *Nature Commun.*, vol. 12, 2021, Art. no. 3141.
[15] F. Lu, G. Li, F. Xiao, and A. Xu, "Compact bidirectional polarization splitting antenna," *IEEE Photon. J.*, vol. 4, no. 5, Oct. 2012.
[16] B. Aqlan *et al.*, "A 300-GHz low-cost high-gain fully metallic Fabry–Perot cavity antenna for 6G terahertz wireless communications," *Sci. Rep.*, vol. 11, 2021, Art. no. 7703.
[17] M. Zucchi *et al.*, "First demonstration of machine-designed ultra-flat, low-cost directive antenna," *Sci. Rep.*, vol. 10, 2021, Art. no. 10506.
[18] A. Hassan, A. Etman, and E. Soliman, "Optimization of a novel nano antenna with two radiation modes using kriging surrogate models," *IEEE Photon. J.*, vol. 10, no. 4, Aug. 2018, Art. no. 4800807.
[19] X. Wang, B. Zhang, W. Wang, J. Wang, and J. Duan, "Design, fabrication, and characterization of a flexible dual-band metamaterial absorber," *IEEE Photon. J.*, vol. 9, no. 4, Aug. 2017, Art. no. 4600512.
[20] H. Huang, Y. Liu, S. Zhang, and S. Gong, "Multiband metamaterial-loaded monopole antenna for WLAN/WiMAX applications," *IEEE Antennas Wireless Propag. Lett.*, vol. 14, pp. 662–665, 2014.
[21] M. Moniruzzaman *et al.*, "Inductively tuned modified split ring resonator based quad band epsilon negative ENG with near zero index NZI metamaterial for multiband antenna performance enhancement," *Sci. Rep.*, vol. 11, 2021, Art. no. 11950.
[22] F. Wan *et al.*, "NGD analysis of turtle-shape microstrip circuit," *IEEE Trans. Circuits Syst. II: Exp. Briefs*, vol. 67, no. 11, pp. 2477–2481, Nov. 2020.

[23] B. Cheng, Z. Du, and D. Huang, "A broadband low-profile multimode microstrip antenna," *IEEE Antennas Wireless Propag. Lett.*, vol. 18, no. 7, pp. 1332–1336, Jul. 2019.
[24] Y. Su, X. Q. Lin, J. W. Yu, and Y. Fan, "Mode composite coplanar waveguide," *IEEE Access*, vol. 7, pp. 109278–109288, 2019.
[25] R. Jackson, "Considerations in the use of coplanar waveguide for millimeter-wave integrated circuits," *IEEE Trans. Microw. Theory Techn.*, vol. 34, no. 12, pp. 1450–1456, Dec. 1986.
[26] N. Zamdmer *et al.*, "Mode-discriminating photoconductor and coplanar waveguide circuit for picosecond sampling," *Appl. Phys. Lett.*, vol. 74, pp. 1039–1041, 1999.
[27] A. Hossain, M. T. Islam, M. E. H. Chowdhury, and M. Samsuzzaman, "A grounded coplanar waveguide-based slotted inverted delta-shaped wideband antenna for microwave head imaging," *IEEE Access*, vol. 8, pp. 185698–185724, 2020.
[28] J. Kaur, Nitika, and R. Panwar, "Design and optimization of a dual-band slotted microstrip patch antenna using differential evolution algorithm with improved cross polarization characteristics for wireless applications," *J. Electromagn. Waves Appl.*, vol. 33, no. 11, pp. 1427–1442, 2019.
[29] A. Okba, T. Alexandru, and A. Herve, "Compact rectennas for ultra-low-power wireless transmission applications," *IEEE Trans. Microw. Theory Techn.*, vol. 67, no. 5, pp. 1697–1707, May 2019.
[30] G. Geetharamani and T. Aathmanesan, "Design of metamaterial antenna for 2.4 GHz wifi applications," *Wireless Pers. Commun.*, vol. 113, pp. 289–2300, 2020.
[31] P. Ramanujam, P. Venkatesan, and C. Arumugam, "Electromagnetic interference suppression in stacked patch antenna using complementary split ring resonator," *Microw. Opt. Technol. Lett.*, vol. 62, pp. 193–199, 2020.
[32] S. Lin *et al.*, "Roll-to-roll production of highly robust 3D-metallized sponge for large-scale high-performance electromagnetic interference shielding," *Adv. Mater. Technol.*, vol. 5, 2020, Art. no. 1900761.
[33] X. Fu, L. Shi, and T. Cui, "Research progress in terahertz metamaterials and their applications in imaging," *J. Mater. Eng.*, vol. 48, no. 6, pp. 12–22, 2020.
[34] V. Trainotti, "Electromagnetic compatibility EMC antenna gain and factor," *IEEE Trans. Electromagn. Compat.*, vol. 59, no. 4, pp. 1006–1015, Aug. 2017.
[35] R. W. Ziolkowski and A. Kipple, "Application of double negative metamaterials to increase the power radiated by electrically small antennas," *IEEE Trans. Antennas Propagations*, vol. 51, no. 10, pp. 2626–2640, 2003.
[36] J. B. Pendry, "Negative refraction makes a perfect lens," *Phys. Rev. Lett.*, vol. 85, pp. 3966–3969, 2000.
[37] Y. Song, Y. Jiao, H. Zhao, Z. Zhang, Z. Weng, and F. Zhang, "Compact printed monopole antenna for multiband WLAN application," *Microw. Opt. Technol. Lett.*, vol. 50, pp. 365–367, 2008.
[38] G. Zhao, F. Zhang, Y. Song, Z. Weng, and Y. Jiao, "Compact ring monopole antenna with double meander lines for 2.4/5 GHz dual-band operation," in *Proc. Prog. Electromagnetics Rearch*, 2007, pp. 187–194.
[39] J. Ranjan and R. S. Kshetrimayum, "An F-shaped printed monopole antenna for dual-band RFID and WLAN application," *Microw. Opt. Technol. Lett.*, vol. 53, no. 7, pp. 1478–1481, 2011.